

# Optimal Sensor Placement for Modal Identification of Bridge Systems Considering Number of Sensing Nodes

Minwoo Chang, S.M.ASCE<sup>1</sup>; and Shamim N. Pakzad, A.M.ASCE<sup>2</sup>

**Abstract:** A series of optimal sensor placement (OSP) techniques is discussed in this paper. A framework for deciding the optimum number and location of sensors is proposed, to establish an effective structural health monitoring (SHM) system. The vibration response from an optimized sensor network reduces the installation and operational cost, simplifies the computational processes for a SHM system, and ensures an accurate estimation of monitoring parameters. In particular, the proposed framework focuses on the determination of the number of sensors and their proper locations to estimate modal properties of bridge systems. The relative importance of sensing locations in terms of signal strength was obtained by applying several OSP techniques, which include effective influence (EI), EI-driving point residue (EI-DPR), and kinetic energy (KE) methods. Additionally, the modified variance (MV) method, based on the principal component analysis (PCA), was developed with the assumption of independence in modal ordinates at each sensing location. Modal assurance criterion (MAC) between the target and interpolated mode shapes from an optimal sensor set was utilized as an effective measure to determine the number of sensors. The proposed framework is verified by three examples: (1) a numerically simulated simply supported beam, (2) finite-element (FE) model of the Northampton Street Bridge (NSB), and (3) modal information identified using a set of wireless sensor data from the Golden Gate Bridge (GGB). These three examples demonstrate the application and efficiency of the proposed framework to optimize the number of sensors and verify the performance of the MV method compared to the EI, EI-DPR, and KE methods. DOI: [10.1061/\(ASCE\)BE.1943-5592.0000594](https://doi.org/10.1061/(ASCE)BE.1943-5592.0000594). © 2014 American Society of Civil Engineers.

**Author keywords:** Structural health monitoring; Optimal sensor placement; Optimal number of sensors; Bridge systems; Modal assurance criteria.

## Introduction

Optimal sensor placement (OSP) is a common issue for all engineering systems for vibration monitoring (Kammer 1990; Yao et al. 1992; Laory et al. 2012). The OSP techniques have been applied to mechanical, aerospace, and structural systems for designing the best sensing locations, which are used to estimate modal parameters based on vibration response. Even though modal parameters were among the early features considered for damage detection, they have proved to be not the most effective damage features, because they are not sensitive to local damage. However, the accurate characterization of modal parameters is important in vibration analysis of structures to calibrate finite-element (FE) models and anticipate dynamic behavior of structures.

As a structural health monitoring (SHM) technique, OSP is considered a challenge for accurate damage identification and estimation of modal parameters (Huston et al. 1994; Morassi and Tonon 2008; Saitta et al. 2008). Advancements in sensing technology, represented by the wireless sensor network (WSN) (Spencer et al. 2004; Lynch and Loh 2006; Pakzad and Fenves 2009), have

facilitated the possibility of vibration monitoring of many structures. However, because the data transmission is a costly task in WSN, maintaining an optimum sensor network size that can still provide the necessary modal information is critical. OSP technique can be utilized efficiently for practical SHM implementations by eliminating redundant sensor data, be it by limiting the number of sensors or by emphasizing which sensors' data should be queried wirelessly for timely modal estimation.

Sensor placement methods examine the information on sensing nodes that are sufficiently sensitive to detect changes in modal parameters (Meo and Zumpano 2005; Cha et al. 2012). The OSP techniques reduce the chance of measuring and processing a large volume of redundant sensor data. Effective influence (EI) method, proposed by Kammer (1990), is one of the most widely used OSP techniques and has been used for many applications (Worden and Burrows 2001; Li et al. 2007, 2011). EI method classifies sensor locations based on the quantified information on observing target modes and eliminates less significant locations from the candidates. To consider the relative contribution of each mode on candidate locations, the driving point residue (DPR) index was introduced and combined with EI method (Papadopoulos and Garcia 1998). Heo et al. (1997) proposed the kinetic energy (KE) method to determine a sensor set that maximizes the KE of the system. Carne and Dohrmann (1995) used the correlation of target mode shapes and defined the sensor set that minimizes the off-diagonal term of correlation matrix. The covariance of target mode shape matrix was utilized for the variance method (Meo and Zumpano 2005), which features the determinant of covariance of the target mode shape matrix as maximized when the optimal sensor configuration is achieved.

The main objective of this study was to develop and validate a new framework for OSP with a minimum number of sensors. In

<sup>1</sup>Graduate Research Assistant, Dept. of Civil and Environmental Engineering, Lehigh Univ., Bethlehem, PA 18015 (corresponding author). E-mail: mic307@Lehigh.edu

<sup>2</sup>P. C. Rossin Assistant Professor, Dept. of Civil and Environmental Engineering, Lehigh Univ., Bethlehem, PA 18015. E-mail: snp208@Lehigh.edu

Note. This manuscript was submitted on June 24, 2013; approved on December 18, 2013; published online on January 27, 2014. Discussion period open until June 27, 2014; separate discussions must be submitted for individual papers. This paper is part of the *Journal of Bridge Engineering*, © ASCE, ISSN 1084-0702/04014019(10)/\$25.00.

general, a large number of sensor nodes are preferred for accurate estimation of modal parameters and effective damage feature extraction for large-scale civil infrastructure. Also, the development of dense WSN and computing technology supports processing a large amount of sensor data. WSN commonly is considered to be cost-effective and convenient for managing a large simultaneous sensor set. The advantage of using WSN for vibration monitoring can be maximized with the integration of OSP technique, which minimizes the cost associated with the installation and synchronization of all wireless sensor units and estimates dynamic characteristics of the structure accurately (Papadimitriou 2004). The OSP techniques also are expected to process sensor data more efficiently and to avoid collecting a large amount of redundant data.

The OSP techniques demonstrate that the accurate estimation of modal parameters can be achieved when the sensors are located properly. In general, the target modes for OSP techniques are selected from preliminary studies, such as FE models or previous field tests, and the sensing locations can be optimized depending on the number of sensors, based on the measure of signal strength at each candidate location. However, the target mode shapes may not be observed accurately from the chosen sensor configuration when the number of sensors is insufficient, sensors are clustered in few regions, or located on modal nodes. To optimize the use of OSP techniques, the minimum number of sensors that is able to characterize the desired mode shapes accurately needs to be identified.

This paper focuses on creating a framework to locate sensors on bridge systems using several OSP techniques and based on the preliminary/previous field tests or FE model. In addition to the existing OSP techniques (including EI, EI-DPR, and KE), a *modified variance* (MV) method is introduced, which is based on the principal component analysis (PCA). The MV method is advantageous for practical implementations by reducing computational tasks for investigating all possible sensor configurations in the variance method. The essence of individual OSP techniques applied in this study is to utilize the optimum sensing locations to identify all targeted modes accurately. Based on the sensor configuration, the mode shapes are interpolated using the spline (Ahlberg et al. 1967) or kriging (Sacks et al. 1989) method. Modal assurance criteria (MAC; Ewins 1984) between the interpolated mode shape from the optimal sensor configuration and the targeted are then used to examine the performance of the chosen sensor configuration. The MAC value is a robust and effective parameter to apply to the preliminary mode shapes, because the error in estimated modes from the FE model or preliminary field tests does not impact it significantly. The number of sensing locations is increased until the subset of sensors estimates target mode shapes with satisfactory accuracy.

To verify this method, it was applied to three examples: (1) a simply supported beam with 19-degrees of freedom (DOF) lumped mass; (2) the Northampton Street Bridge (NSB), which has 42 candidate sensing locations; and (3) the Golden Gate Bridge (GGB) modal identified using ambient vibration data from 46 wireless sensing units.

## Framework of Optimal Number of Sensors in Bridge System

The objective of the optimization problem is to minimize the number of sensors and to locate them properly for the quality estimation of target dynamic modes in bridge structures. In particular, vertical and torsional modes are targeted together, so that the optimal sensor configuration is suitable to monitor all mode shapes usually associated with vertical response. The optimal number of sensors and their locations are expected to simultaneously produce the minimum

sensor management cost as well as accurate estimation of structural modal parameters.

Several OSP techniques were applied to define the best sensing locations, suitable for observing target mode shapes associated with the number of sensors. As a common criterion to decide the number of sensors in this study, the MAC value between the interpolated (from an optimal sensor configuration) and target mode shapes was used. For an individual subset of sensors, curve-fitting methods [spline (Ahlberg et al. 1967) and kriging (Belytschko et al. 1994)] were applied to interpolate modal ordinates at locations that were excluded from the candidate locations. The following is a brief description of the investigated interpolation methods.

### Spline Interpolation

The spline is a widely used curve-fitting method that minimizes total curvature and maximizes straightness of the approximated shape (Ahlberg et al. 1967). The modal ordinates for the nonmeasurable or nonmeasured locations are interpolated by using the piecewise  $p$ th order of spline, which minimizes the residual sum of squares,  $S$ , defined as

$$S = \sum_i [y_i - s(x_i)]^2 \quad (1)$$

where  $x_i$  =  $i$ th sensing location;  $y_i$  = corresponding sensor data; and  $s$  =  $p$ th order of polynomial function for each segment. The compatibility equations are defined by using the continuities of entire shape function at sensor locations up to  $(p - 1)$ th derivatives. To compensate the unknown coefficients for piecewise polynomial functions, the additional modal ordinates are extrapolated linearly for the outside of the investigated span. Using the continuity of modal ordinates as well as their derivatives, the continuous piecewise functions are determined.

### Kriging Interpolation

The kriging method estimates a shape function that minimizes the error of the spatial predictions (Belytschko et al. 1994). A kriging model is defined as a weighted sum of known neighbors and indicates a geostatistical estimator, which fits well with real mode shapes. The shape function is initially estimated by a linear regression model with random error  $z(x_i)$  as

$$y_i = \mathbf{p}(x_i)^T \mathbf{a} + z(x_i) \quad (2)$$

where  $\mathbf{p}(x_i)$  = a set of nonlinear basis, dependent on geometric information of  $x_i$ , e.g.,  $\mathbf{p}(x_i)^T = [1 \quad x_i]$  for linear basis;  $\mathbf{a}$  = coefficient vector that minimizes the error of predictor; and  $z(x_i)$  = realization of a stochastic process with zero mean and a nonzero covariance. The covariance matrix of  $z(x)$  is defined by the correlation between modal ordinates at two locations. Gaussian function frequently is used to reflect high correlation for closely located sensors as

$$R(x_i, x_j) = \exp(-\theta r_{ij}^2) \quad (3)$$

where  $\theta$  = predefined correlation parameter; and  $r_{ij}$  = physical distance between  $x_i$  and  $x_j$ . This is an appropriate choice, because a Gaussian function is simple and convenient to model correlation that smoothly decreases as the relative distance increases. The mode shape is estimated using the best linear unbiased prediction of  $\mathbf{a}$ . To formulate a well-conditioned  $\mathbf{R}$  matrix, the optimal value of correlation parameter should be defined. In this study, the correlation parameter,

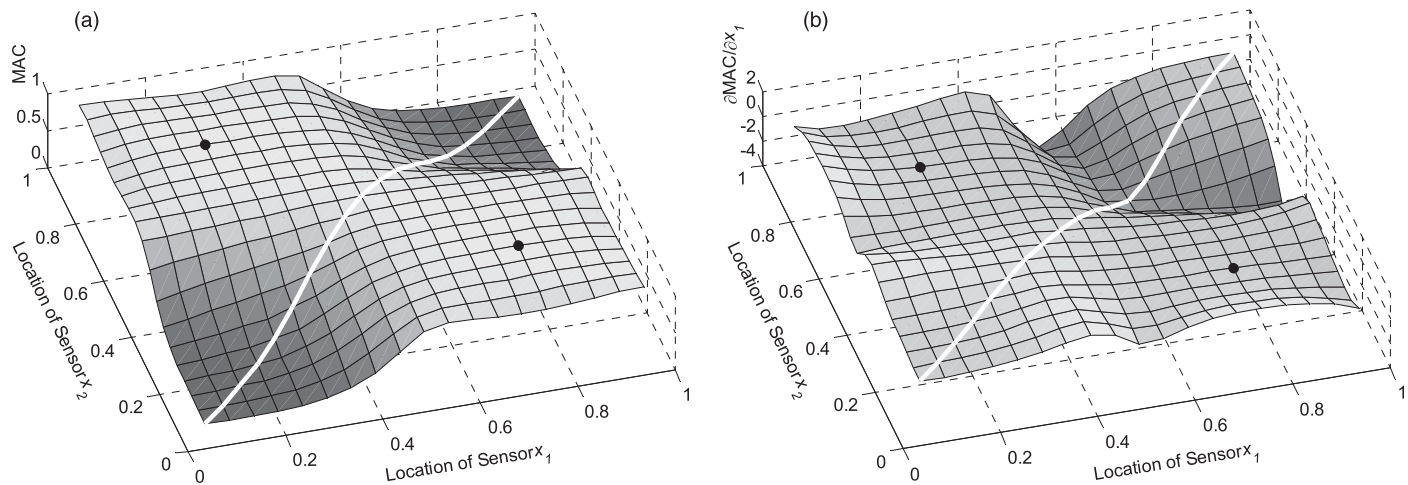


**Fig. 1.** 3D contour of (a) MAC and (b)  $\partial \text{MAC} / \partial x_i$  when two sensors are located on a simply supported beam model to observe a sinusoidal mode shape

$\theta$ , is iteratively controlled to place eigenvalues of the covariance matrix within interval  $[10^{-6}$  to  $10^{-1}]$ , which promises quality estimation of shape function based on the parametric analysis (Gu 2003).

### MAC Comparison

MAC for the  $i$ th target mode between an estimated mode shape vector with interpolation ( $\bar{\varphi}$ ) and an exact mode shape ( $\hat{\varphi}$ ) is calculated as

$$\text{MAC}_i = \frac{|\bar{\varphi}^T \hat{\varphi}|}{\sqrt{(\bar{\varphi}^T \bar{\varphi})(\hat{\varphi}^T \hat{\varphi)}}} \quad (i = 1, 2, \dots, \bar{N}) \quad (4)$$

where  $\bar{N}$  = number of target modes.

To examine the MAC variation, its sensitivity with respect to sensor locations was investigated and the contour plots for MAC and its derivative were visualized. A MAC value between the estimated mode shape  $\hat{\varphi}(x)$  and the exact mode shape  $\phi(x)$  associated with vertical vibration for bridge structures can be defined as a function of sensor locations  $(x_1, x_2, \dots, x_N)$  as

$$\text{MAC}(x_1, x_2, \dots, x_N) = \frac{\sum_{i=0}^N \int_{x_i}^{x_{i+1}} [\phi(x) \cdot \hat{\varphi}_i(x)] dx}{\sqrt{\int_{x_0}^{x_{N+1}} [\phi(x)]^2 dx} \sqrt{\sum_{i=0}^N \int_{x_i}^{x_{i+1}} [\hat{\varphi}_i(x)]^2 dx}} \quad (5)$$

The maxima of Eq. (5) can be obtained by searching its zero derivatives. For example, if the true mode shapes are sinusoidal (as is the case for a simple beam with distributed mass and elasticity), the problem of finding the optimal locations for any two sensors has two solutions, which correspond to its zero derivatives; these solutions occur when  $\mathbf{x} = [0.25 \ 0.75]$  or  $\mathbf{x} = [0.75 \ 0.25]$ , as shown in contour plots (Fig. 1). In the same manner, the best sensor configuration to maximize MAC for higher modes was investigated with additional sensors and the corresponding MAC values are noted (Table 1). Additionally, a MAC value was estimated when an equal number of sensors were uniformly spaced. The results indicated that the interpolation accurately approximates target mode shape better when the sensors are located properly.

**Table 1.** Best Sensor Configuration to Observe Harmonic Mode Shape Using Cubic Spline and Comparison of MAC to Uniformly Spaced One

| Mode | Sensor location to maximize MAC   | MAC              |                 |
|------|-----------------------------------|------------------|-----------------|
|      |                                   | Optimal solution | Uniform spacing |
| 1    | 0.500                             | 0.9999           | 0.9999          |
| 2    | 0.250, 0.750                      | 0.9999           | 0.9980          |
| 3    | 0.167, 0.500, 0.833               | 0.9999           | 0.9916          |
| 4    | 0.138, 0.362, 0.639, 0.862        | 0.9997           | 0.9810          |
| 5    | 0.121, 0.288, 0.500, 0.712, 0.879 | 0.9991           | 0.9677          |

The error of MAC is defined as a measure of accuracy associated with the number of sensors as

$$\epsilon_{\text{MAC}} = 1 - \min(\text{MAC}) \quad (6)$$

All target modes were considered as identified when  $\epsilon_{\text{MAC}}$  was smaller than the desired level; otherwise, an extra sensor was added on the next configuration and the comparison task was repeated.

Because the closed-form solution to obtain maximum MAC is applicable only for the low-dimensional problems owing to heavy computational tasks, the OSP techniques should provide an effective way to search for the best sensor configuration with efficient computational cost. The minimum number of sensors is determined when the criteria for minimum error of MAC are satisfied. The entire procedure is organized in Fig. 2.

### Optimal Sensor Placement

The OSP techniques in this study play a key role of ranking sensing locations based on the relative importance to monitor target modes, which can be conducted by the following methods: (1) EI, (2) EI-DPR, and (3) KE. As an alternative approach, the MV method is introduced based on the PCA. The theoretical backgrounds of these four OSP techniques are described subsequently.

#### EI Method

Kammer (1990) proposed the EI method for searching the best locations with  $N$  number of sensors. The Fisher information matrix (Middleton 1960) associated with candidate sensing locations is

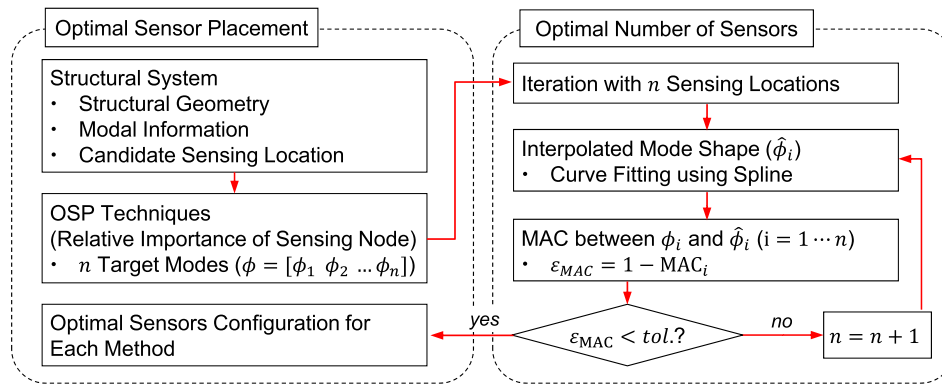


Fig. 2. Framework for determining the best sensor configuration

evaluated for target modes and, then, used to maximize the spatial independence by ranking the contribution of each sensing location.

The vibration response,  $y$ , measured from the structure can be estimated with the combination of the contribution of  $m$  target modes as

$$\mathbf{y} = \Phi \mathbf{q} + \mathbf{w} \quad (7)$$

where  $\Phi \in \mathbb{R}^{n \times m}$  = target mode shape matrix obtained from FE model with  $n$  = number of the candidate sensing locations;  $\mathbf{q}$  = modal contribution factor associated with  $m$  target modes; and  $\mathbf{w}$  = stationary random noise vector with a mean of zero.

An unbiased estimator  $\hat{\mathbf{q}} = (\Phi^T \Phi)^{-1} \Phi^T \mathbf{y}$  is used to evaluate the error in the estimation of vibration response. The numeric deployment shows that the covariance of the error between the modal contribution factor  $\mathbf{q}$  and the unbiased estimator  $\hat{\mathbf{q}}$  is identical to the inverse of the Fisher information matrix  $\mathbf{F}$  as

$$\mathbf{J} = E[(\mathbf{q} - \hat{\mathbf{q}})(\mathbf{q} - \hat{\mathbf{q}})^T] = \left(\frac{1}{\sigma^2} \Phi^T \Phi\right)^{-1} = \mathbf{F}^{-1} \quad (8)$$

where  $\sigma$  = variance of the stationary random noise vector,  $\mathbf{w}$ . The Fisher information matrix measures the amount of information that the mode shape matrix carries for a specific sensor set. Therefore, the best estimation  $\hat{\mathbf{q}}$  is achieved when a Fisher information matrix,  $\mathbf{F}$ , is maximized.

The EI method solves this optimization problem by examining the contribution of the candidate sensor nodes and truncating sensor positions that lower the determinant of  $\mathbf{F}$ . For evaluating the contribution of the candidate sensor locations, the effective independence distribution (EID) vector,  $\mathbf{E}_D$ , is introduced as (Kammer 1990)

$$\mathbf{E}_D = [\Phi \boldsymbol{\psi}] \otimes [\Phi \boldsymbol{\psi}] \cdot \boldsymbol{\lambda}^{-1} \mathbf{1} \quad (9)$$

where  $\boldsymbol{\psi}$  and  $\boldsymbol{\lambda}$  = eigenvector and eigenvalue of  $\mathbf{F}$ , respectively;  $\mathbf{1}$  = column vector composed of  $m$  unity values to sum all fractional contribution corresponding to target modes at each sensor location; and  $\otimes$  = term-by-term matrix multiplication, which transforms the dot product  $\Phi \boldsymbol{\psi}$  into absolute identification space to quantify modal contribution at each sensor location.

The  $i$ th element of  $\mathbf{E}_D$  indicates the fractional contribution at  $i$ th sensor location when all target modes are considered to be equally important. A sensor location that is noted as a lowest index of  $\mathbf{E}_D$  is discarded from the candidate locations, and this procedure is repeated until the candidate location is a null value and the priority of sensor locations is determined.

### EI-DPR Method

The DPR coefficient was introduced previously to enhance the EI method (Papadopoulos and Garcia 1998). The limitation of the EI method, which allows selecting sensor locations associated with low energy content, is avoided by multiplying the DPR coefficient for each element of a fractional contribution vector. The newly described EID vector ( $\mathbf{E}_{D\_DPR}$ ) is calculated as

$$\mathbf{E}_{D\_DPR} = ([\Phi \boldsymbol{\psi}] \otimes [\Phi \boldsymbol{\psi}] \cdot \boldsymbol{\lambda}^{-1} \mathbf{1}) \otimes \mathbf{DPR} \quad (10)$$

In Eq. (10), the  $i$ th element of  $\mathbf{DPR}$  is given by

$$\mathbf{DPR}_i = \sum_{j=1}^m \frac{\phi_{ij}^2}{\omega_j} \quad (11)$$

where  $\phi_{ij}$  = modal coordinate for  $j$ th mode at  $i$ th location; and  $\omega_j$  =  $j$ th modal frequency. The DPR coefficient is a weighting factor that considers relative modal contribution on each sensing location to evaluate EID vector. Consequently, EI-DPR method concentrates the sensors on the high energy content regions.

### KE Method

Heo et al. (1997) proposed the KE method, which is similar to EI in the procedure but directly involves the mass of the system. KE method is supposed to maximize the KE instead of the Fisher information matrix of the EI and EI-DPR methods. The KE matrix  $\mathbf{P}$  is defined as

$$\mathbf{P} = \Phi^T \mathbf{M} \Phi \quad (12)$$

where  $\mathbf{M}$  = mass of the structure. The KE matrix can be expressed as the dot product of matrix  $\boldsymbol{\Psi}$  and its transpose by decomposing the mass matrix into the lower ( $\mathbf{L}$ ) and upper ( $\mathbf{U}$ ) triangular Choleski factor matrices as

$$\mathbf{P} = \boldsymbol{\Psi}^T \boldsymbol{\Psi} \quad (13)$$

where  $\mathbf{M} = \mathbf{L}\mathbf{U}$ ; and  $\boldsymbol{\Psi} = \mathbf{U}\Phi$ . Similar to the Fisher information matrix in EI method, the KE matrix can be considered as a measure of the amount of information in target mode shape matrix with the weighting factor of  $\mathbf{U}$ . The rest of the procedures, repeating the truncation of sensing locations from the candidate, are similar to the EI method.



## MV Method

The proposed MV method utilizes PCA, which transforms a set of observed data into uncorrelated variables such that the greater variable indicates the more informative component. The covariance matrix is a widely used mathematical tool to estimate the correlation between associated variables. Fedorov and Hackl (1994) studied the most informative subset using covariance analysis from randomly distributed observation. Variance method, based on the most informative subset technique, has been developed to locate sensors on the bridge systems by using the independency of modal ordinates at each sensing location (Meo and Zumpano 2005). To estimate the signal strength of the investigated sensor configuration, the  $vr$  index is introduced, estimating signal strength by normalizing the diagonal element by the sum of off-diagonal elements. Although variance method reduces computational cost by avoiding the determinant estimation, it is still computationally expensive because signal strengths should be estimated for all possible subsets. The total number of subsets of target mode shapes,  $N_c$ , is defined as

$$N_c = \sum_{k=1}^{n-1} \binom{n}{k} = \sum_{k=1}^{n-1} \frac{n!}{k!(n-k)!} \quad (14)$$

where  $k$  = number of sensors, which is usually unknown for OSP. The number of possible subsets, which is a function of candidate sensor locations, increases greater than exponentially.

In this study, a new OSP technique that is based on PCA is proposed. This method performs better than the variance method with relatively light computational cost for high-dimensional problems. The mode shape data, used to calculate covariance matrix, are transformed into  $\Psi = [\Phi^T \quad -\Phi^T]^T$  to prevent the irregularity in covariance matrix from the biased sign convention for each mode and to increase independency of modal information in each sensing location. The observable modal ordinates from  $p$  locations,  $\Psi_p^T = [\Phi_p^T \quad -\Phi_p^T]$ , are used to evaluate the linearly estimated modal ordinates  $\hat{\Psi}_q^T = [\hat{\Phi}_q^T \quad -\hat{\Phi}_q^T]$  for the rest of  $n - p$  locations as (Fedorov and Hackl 1994)

$$\hat{\Psi}_q^T = C_{qp} C_{pp}^{-1} \Psi_p^T \quad (15)$$

where  $q = n - p$ ; and  $C_{qp}$  and  $C_{pp}$  = block matrices that are the submatrix of the covariance of the total target mode shape matrix  $\Psi^T = [\Psi_p^T \quad \Psi_q^T]$ , which yields

$$\text{cov}(\Psi^T) = \begin{bmatrix} C_{pp} & C_{pq} \\ C_{qp} & C_{qq} \end{bmatrix} = \begin{bmatrix} \text{cov}(\Psi_p^T) & C_{pq} \\ C_{qp} & \text{cov}(\Psi_q^T) \end{bmatrix} \quad (16)$$

The error in the unbiased estimator is minimized when the determinant of  $C_{pp}$  is maximized (Fedorov and Hackl 1994). For the invertible  $C_{pp}$ , the number of sensors is at least equal to the number of target modes so that the zero eigenvalue is avoided.

The independence of modal parameters at each sensing location theoretically formulates a diagonal matrix for  $\text{cov}(\Psi^T)$  as well as its submatrix  $C_{pp}$ . As noted before, the independence between modal ordinates from two sensing locations is enhanced by assembling target mode matrix with original mode shape and its negative. The signal strength of the candidate sensing location can be represented by the diagonal element of  $\text{cov}(\Psi^T)$ , while the off-diagonal elements are considered as noise parameters.

For the practical implementations, the  $pc$  index is introduced to evaluate the signal strength at each sensing node with consideration for the dispersion of off-diagonal coefficients as

$$pc_i = \frac{c_{ii}}{\sqrt{\sum_{j=1, j \neq i} c_{ij}^2}} \quad (17)$$

where  $c_{ij}$  =  $i$ th row and  $j$ th column of the covariance matrix. The sensor location with the lowest signal strength vanishes from the candidate sensor locations and this procedure is repeated for the reduced size of target mode matrix.

## Case Studies

Three examples were used to verify the performance of the proposed OSP technique and to define the optimal number of sensors: (1) a numerically simulated, 19-DOF, simply supported beam with lumped masses on each node; (2) NSB with 42 candidate sensing locations; and (3) GGB with 46 vertical wireless sensors. In addition to the verification of the proposed framework, the simply supported beam model was used to compare the performance of the MV method to existing methods and exact solution, which require heavy computational tasks. The NSB example investigated the effect of symmetric condition for OSP in bridge systems and different levels of MAC. The preliminary field test result was used for the GGB example, and the effect of interpolation methods is discussed.

### Simply Supported Beam

This example verified the performance of the MV method and compared it to results from the variance method and the exact solution, which maximizes the determinant of covariance matrix. A 19-DOF, lumped mass system was designed numerically for a simply supported beam model. The unit mass was distributed on the equally spaced, 19 candidate sensing locations, and the dynamic condensation was applied to monitor vertical modes. The submatrix, which maximizes its determinant depending on the number of sensors, was compared to results from the MV method. Spline fitting was used for both methods to interpolate mode shapes.

Table 2 shows the best sensing locations depending on the number of sensors when the first five dynamic modes are targeted. Because the rank of the covariance matrix usually is determined as equal to the number of target modes, at minimum the equivalent number of sensing locations, which was five for this example, theoretically are required to collect sufficient information in the optimal sensor configuration. The results in Table 2 indicate that the sensor configurations for MV identifies the same sensor configuration with almost uniform spacing as the exact solution when five sensors are placed, whereas variance method shows a different sensor configuration.

The significant advantage of the MV method is the reduction of computational cost via elimination of candidate sensor location one by one (instead of investigation of all possible sensor configurations). The computational efficiency was compared by estimating the total number of operations, which is a function of the number of candidate sensor locations and the number of target modes. Fig. 3 shows the number of operations in logarithmic scale when the number of target modes is varied, and demonstrates that the MV method is computationally more efficient than others. Considering that this result excludes the memory allocation process for large memory storage, the MV method is more efficient in maintaining accurate search for principal component and practically applicable for many engineering systems associated with dense sensor networks.

Further information is contained in the error of minimum MAC among the target modes in logarithmic scale versus the number of

**Table 2.** Sensor Configuration Comparison for 19-DOF, Simply Supported Beam with Lump Mass

| Number of sensors | Sensor locations |   |   |   |   |    |   |   |   |   |          |   |   |   |   |   |
|-------------------|------------------|---|---|---|---|----|---|---|---|---|----------|---|---|---|---|---|
|                   | Exact solution   |   |   |   |   | MV |   |   |   |   | Variance |   |   |   |   |   |
| 1                 | X                |   |   |   |   |    |   |   |   |   |          |   |   |   |   | X |
| 2                 | X                |   |   |   |   | X  |   |   |   |   |          |   |   |   | X | X |
| 3                 | X                |   | X |   |   | X  |   |   |   |   |          |   |   | X | X | X |
| 4                 | X                | X | X |   |   | X  |   | X |   |   |          |   | X | X | X | X |
| 5                 | X                | X | X | X |   | X  |   | X |   | X |          | X | X | X | X | X |
| 6                 | X                | X | X | X | X | X  |   | X | X | X |          | X | X | X | X | X |
| 7                 | X                | X | X | X | X | X  | X | X | X | X |          | X | X | X | X | X |
| 8                 | X                | X | X | X | X | X  | X | X | X | X | X        | X | X | X | X | X |

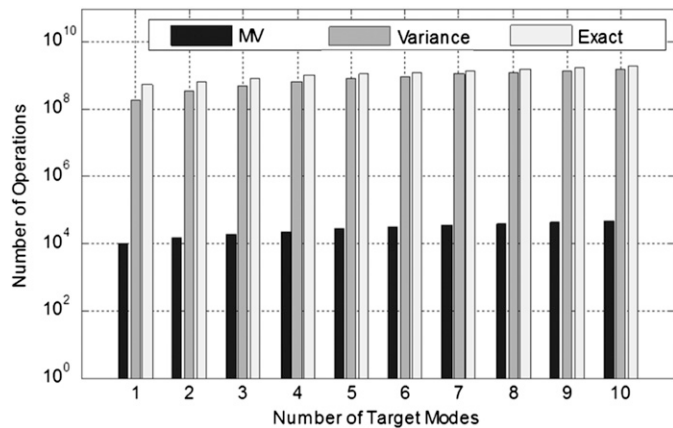


**Fig. 3.** Comparison of number of operations in MV and variance methods with exact solution

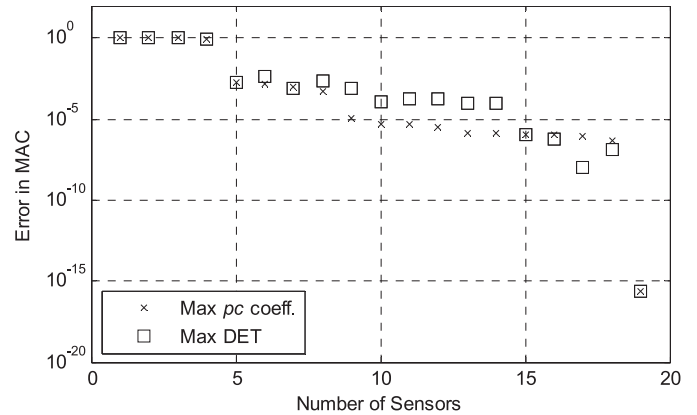


**Fig. 4.** Error in minimum MAC among target modes for MV method (X) and exact solution (open square)

active sensors (Fig. 4). It shows that mode shapes can be estimated using five sensors with more than 99% agreement in MAC. Because of the zero eigenvalues, the error of MAC after six sensor locations was random for the maximum determinant of covariance matrix, while it decreased monotonously for the MV method.

The proposed framework for the optimal number of sensors was applied to analyze the performance of OSP methods including EI, EI-DPR, KE, as well as the MV method. All mode shapes were interpolated using kriging method and the MAC threshold of 0.99 was used. Except EI-DPR, all investigated methods showed the linear increase in the number of sensors owing to an increase in the target modes (Fig. 5).

**Northampton Street Bridge**

The NSB, which connects Easton, Pennsylvania, to Phillipsburg, New Jersey, across the Delaware River, was used for the application of OSP considering the number of sensors. The NSB is a cantilever truss bridge with a total span length of 170.688 m (560 ft) supported by two piers. The main span of the bridge is composed of nine stringers that are crossed by floor beams. To observe modal parameters of the bridge, the FE model of the bridge was built in SAP2000 with 375 truss elements and 265 nodes. Fig. 6 shows the plan and elevation views of the NSB and the 21 candidate sensing locations on both north and south sides (rectangular shape markers). In this study, vertical and torsional modes were considered as target modes, of which the first five are shown in Fig. 7 with their natural frequencies.

The four OSP techniques were applied to determine both the optimal number of sensors and their best sensing locations. The

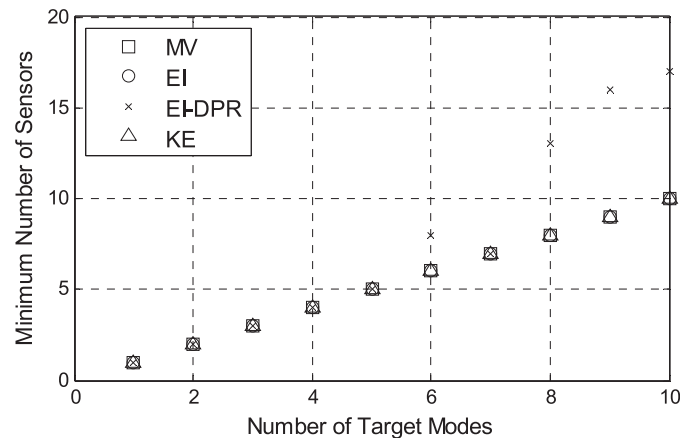


**Fig. 5.** Optimal number of sensors for 19-DOF, simply supported beam using MV, EI, EI-DPR, and KE methods

results by OSP showed almost symmetric sensor configurations in the longitudinal direction. (A particular case of sensor configuration is shown subsequently.) For this example, the mode shapes for north and south sides were interpolated separately using spline based on the OSP results. Figs. 8(a and b) show the required number of sensors versus the number of target modes for the MAC thresholds of 0.9 and 0.95, respectively. The optimal numbers of sensors generally did not increase linearly as the number of target modes increased. All methods recorded a similar performance when the number of target modes was less than five regardless of MAC thresholds. The reduced

number of sensor locations suggested that the better estimation of signal strength was achieved with the higher target modes. This provided more opportunities to minimize the number of sensors and monitor more modal information. By including the higher modes in the target modes, a better optimization result was achieved. This effect was more frequent when the MAC threshold was 0.95, which

occurred when the preliminary study/FE model could provide an accurate estimate of these modes. Because the MAC comparison only was required for the target modes, the optimal number of sensors could be reduced further; for example, the optimal number of sensors for the KE method to estimate three target modes could be 11 or fewer, instead of 15.

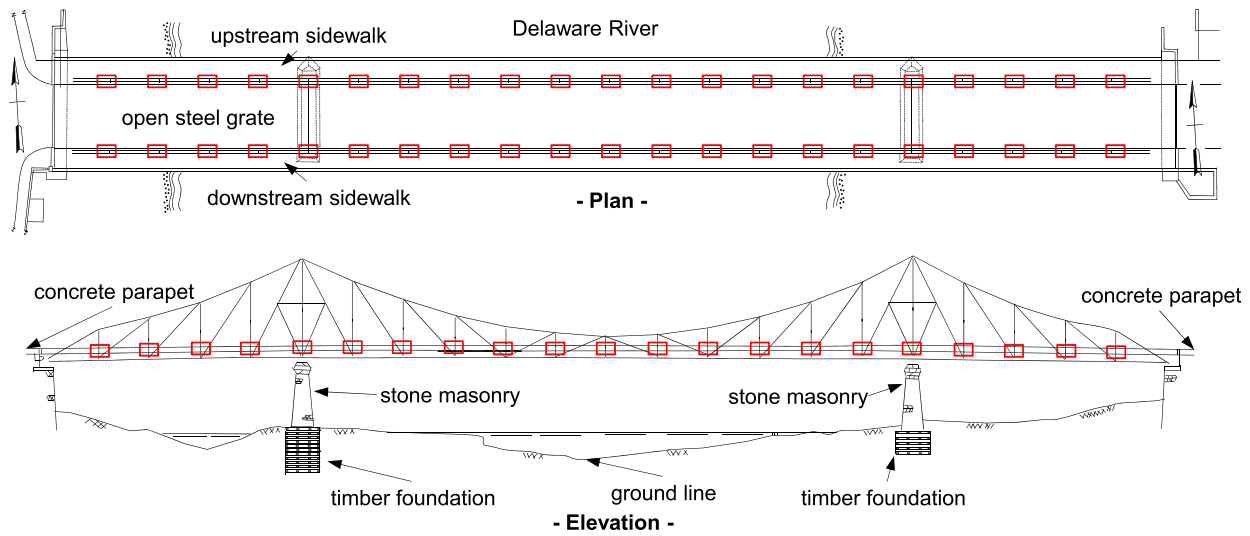


Fig. 6. Plan and elevation views of NSB with 42 candidate sensor locations

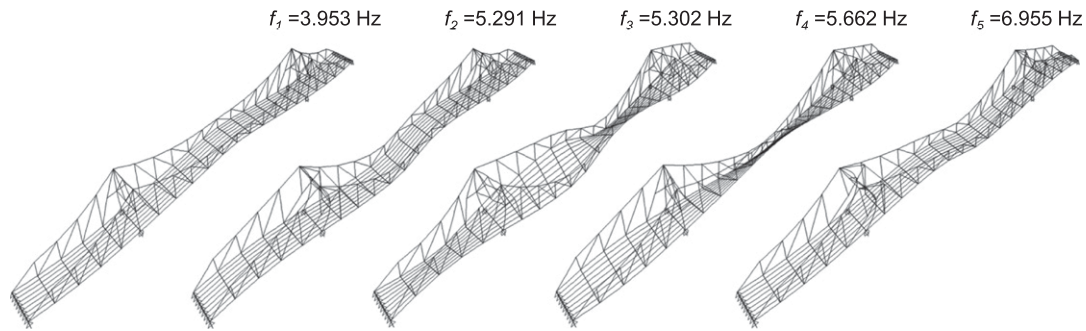


Fig. 7. First five estimated mode shapes (three vertical and two torsional) of NSB

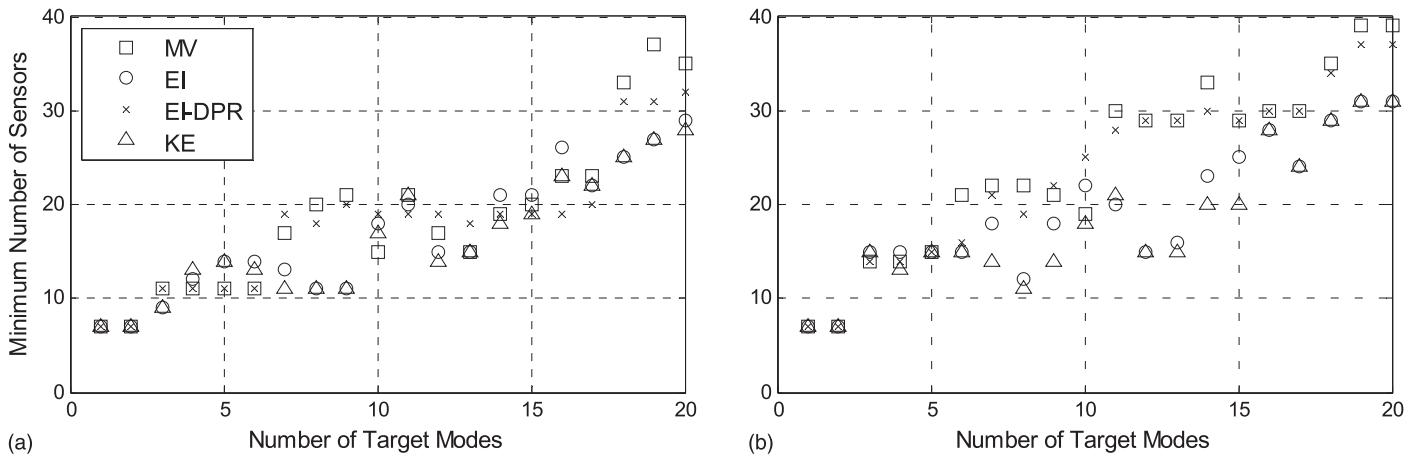


Fig. 8. Number of sensors for each number of target modes for NSB: (a) MAC = 0.90; (b) MAC = 0.95

To investigate the actual sensor configuration depending on the method, the sensor locations were plotted for a particular scenario in which five modes were targeted and the MAC threshold was set to 0.95 (Fig. 9). To investigate the effect of OSP methods, the target modes were not expanded. All methods commonly determined 15 sensing locations as an optimal solution: the MV method [Fig. 9(a)] located sensors symmetrically on both sides of the north and south as well as the east and west with fairly uniform spacing; the EI method [Fig. 9(b)] and KE method [Fig. 9(d)] showed similar sensor configuration with fairly uniform spacing; and the EI-DPR method [Fig. 9(c)] concentrated sensor locations on the middle of the main span and no sensors on either side spans. This sensor configuration was focused on the lower modes. Theoretically, the DPR parameter gives more weight (because of high impact) for very low modes compared to EID vector of the EI method. As noted in the OSP results and sensor configuration plots, OSP methods estimated a least informative location sequentially from both sides of the bridge. Depending on the mode shape information and applied method, this procedure resulted in nonsymmetric configurations for both sides of the bridge. It implies the importance of investigating signal strength from both sides of a bridge structure for accurate mode shape estimation, and is practically useful when nonsymmetric behavior is observed or expected from the preliminary tests.

### Golden Gate Bridge

The MV method was verified using the dynamic modes from the GGB identified from ambient vibration data. Pakzad and Fenves (2009) used a WSN to measure acceleration data from 65 wireless sensing units, and identified 25 vertical, 19 torsional, and 23 transverse modes on the main span of the bridge using the autoregressive (AR) method (Pandit 1991). To distinguish the vertical and torsional modes that are coupled in the vertical response, three reference nodes were installed on the opposite side of the bridge (east side). In this application, vertical and torsional modes were targeted using modal ordinates from the 46 candidate locations on the west side of the bridge. For estimating modal parameters of the bridge, structural modal identification toolsuite (SMIT; Chang and Pakzad 2013) was used to analyze vertical acceleration response.

This example aimed to verify the best sensor configuration using modal parameters from system identification and to compare the performance of investigated interpolation techniques. Figs. 10(a and b) show the number of required sensors for each method versus the number of target modes with the MAC thresholds of 0.95 when both spline and kriging interpolation methods, respectively, were used to observe mode shapes. Generally, the minimum number of sensors increased linearly as the additional modes were targeted. The MV method produced the smallest minimum number of sensors for most

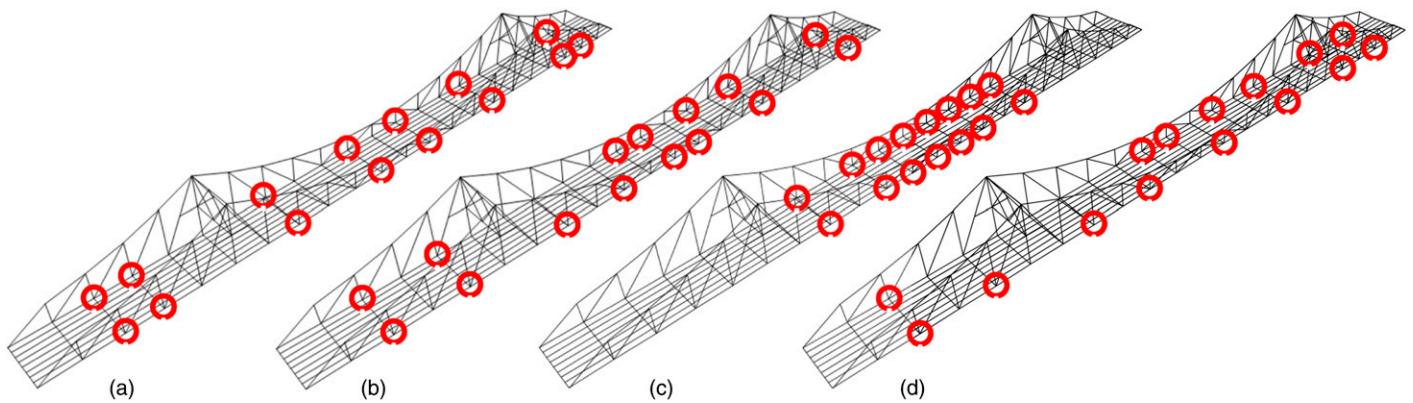


**Fig. 9.** Optimal sensor configuration when the first five modes are targeted from the FE model of NSB; 15 sensors for all investigated methods including (a) MV, (b) EI, (c) EI-DPR, and (d) KE methods

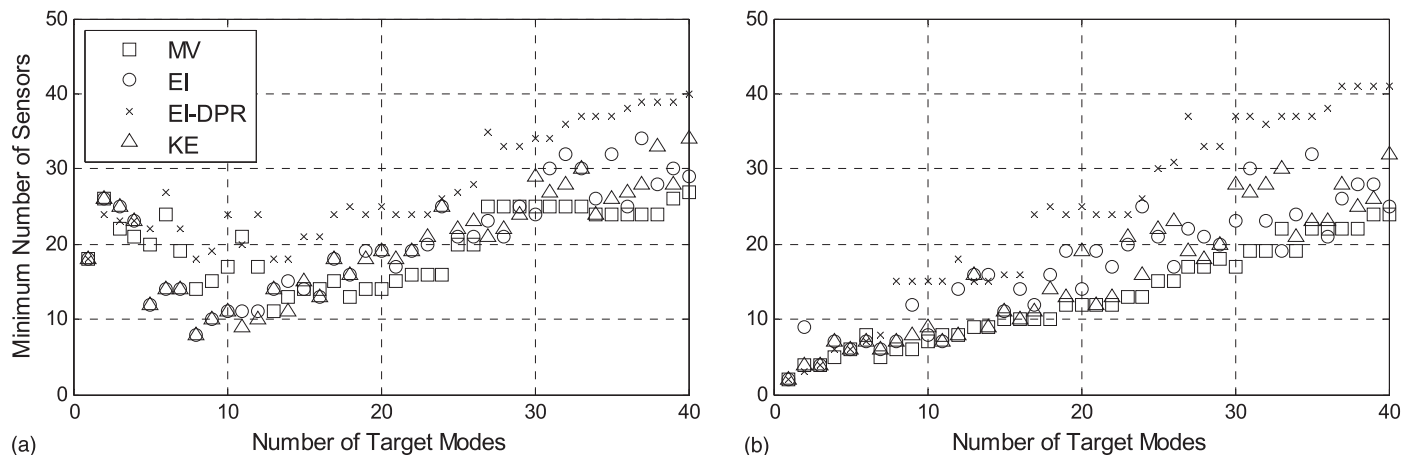


**Fig. 10.** Number of sensors for each number of target modes of GGB for MAC threshold of 0.95: (a) spline; (b) kriging



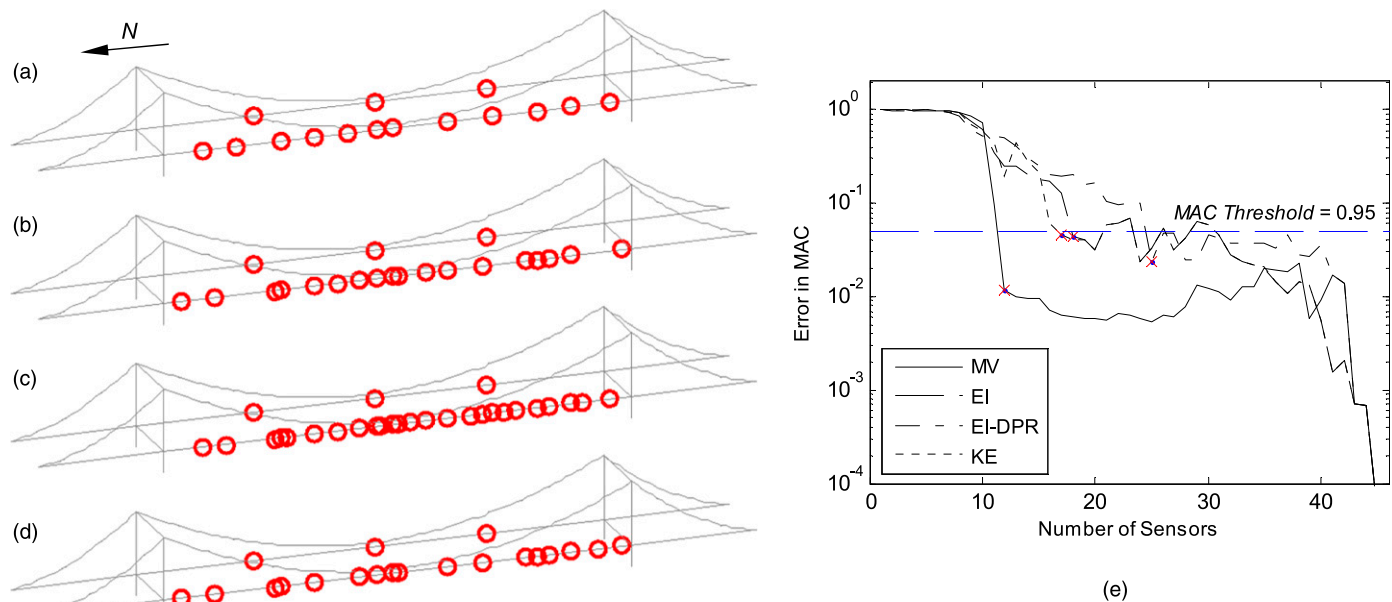


**Fig. 11.** OSP results when 20 modes of GGB are targeted: (a) MV with 12 sensors; (b) EI with 18 sensors; (c) EI-DPR with 25 sensors; (d) KE with 17 sensors on west side of GGB; (e) error of minimum MAC changes for the number of sensors

scenarios. Also, kriging interpolation showed better performance than spline in determining the number of sensors. For both interpolation methods, the minimum number of sensors decreased as target modes increased, regardless of OSP methods, when a low number of modes were targeted. This indicates that the signal strength at candidate sensing locations was evaluated incorrectly owing to insufficient information of mode shape matrix.

The results of OSP were utilized to determine the minimum number of sensors using MAC comparison for any specific number of target modes. Fig. 11 shows the optimal sensor configurations for all investigated methods when 20 modes were targeted. The required number of sensors for the MV method was 12 when kriging interpolation with the MAC threshold of 0.95 was used, which showed a better performance in minimizing the number of sensors compared to the EI, EI-DPR, and KE methods. The maximum error of MAC for each method is plotted [Fig. 11(e)], with the number of sensors to satisfy the given MAC threshold marked.

## Conclusion

In this paper, a framework to optimize the number of sensors and their locations for bridge systems is proposed. The OSP techniques were integrated with the proposed framework to analyze the best sensor configuration. All investigated OSP techniques evaluated signal strength for candidate sensing locations, and the results were used to reconstruct the dynamic mode shapes as they were targeted using the minimum number of sensors. As a criterion to determine the minimum number of sensors, a MAC value between the exact and the estimated mode shapes was used.

Several OSP methods were applied to quantify the signal strength for candidate sensor nodes. In addition to the existing OSP methods, the MV method was developed to estimate signal strength from the covariance of transformed mode shape matrix. The MV method successfully determined priority of sensing locations, and proved more effective compared to the variance method and exact solution using the simply supported beam example. The computational cost comparison showed that the MV method is more practical for sensor

placement in engineering systems instrumented with a large sensor network.

The results of OSP methods for NSB showed similar performance for all investigated methods in terms of the minimum number of sensors. The EI-DPR method concentrated sensors on the mid-span, whereas the EI, KE, and MV methods located sensors with almost uniform spacing. The most effective OSP method for specific target modes depended on the level MAC threshold, for which engineering judgment is required, to place the optimal number of sensors in the proper locations. A nonlinear relationship between the numbers of target modes and the number of sensors was observed, which provided more opportunities to minimize the number of sensors when higher modes were estimated from the preliminary study/FE model.

The implementation of modal parameters for GGB verified that the preliminary field test was used effectively to monitor the vibration of the bridge. Two techniques (spline and kriging) were investigated to interpolate mode shapes from the selected locations. Spline assumes the boundary conditions to connect piecewise components and kriging requires a priori information for the covariance of a stochastic process. The results from the analysis of GGB indicated kriging was more effective to estimate mode shapes accurately. For this example, the MV method performed better compared to others in terms of number of sensors.

## Acknowledgments

This research was partially supported by National Science Foundation under grant CMMI-0926898 by the Sensors and Sensing Systems program, and by a grant from the Commonwealth of Pennsylvania, Department of Community and Economic Development, through the Pennsylvania Infrastructure Technology Alliance (PITA).

## References

Ahlberg, J. H., Nilson, E. N., and Walsh, J. L. (1967). *The theory of splines and their applications*, Academic Press, New York.

- Belytschko, T., Lu, Y. Y., and Gu, L. (1994). "Element-free Galerkin methods." *Int. J. Numer. Methods Eng.*, 37(2), 229–256.
- Carne, T. G., and Dohrmann, C. R. (1995). "A modal test design strategy for model correlation." *Proc., 13th Int. Modal Analysis Conf.*, Society for Experimental Mechanics (SEM), Bethel, CT.
- Cha, Y. J., Agrawal, A. K., Kim, Y., and Raich, A. M. (2012). "Multi-objective genetic algorithms for cost-effective distributions of actuators and sensors in large structures." *Expert Syst. Appl.*, 39(9), 7822–7833.
- Chang, M., and Pakzad, S. N. (2013). "Observer Kalman filter identification for output-only systems using interactive structural modal identification tool suite." *J. Bridge Eng.*, 10.1061/(ASCE)BE.1943-5592.0000530, 04014002.
- Ewins, D. J. (1984). *Modal testing: Theory and practice*. Research Studies Press, Letchworth, Hertfordshire, U.K.
- Fedorov, V. V., and Hackl, P. (1994). "Optimal experimental design: Spatial sampling." *Calcutta Statistical Assoc. Bull.*, 44(173–174), 57–81.
- Gu, L. (2003). "Moving kriging interpolation and element-free Galerkin method." *Int. J. Numer. Methods Eng.*, 56(1), 1–11.
- Heo, G., Wang, M. L., and Satpathi, D. (1997). "Optimal transducer placement for health monitoring of long span bridge." *Soil. Dyn. Earthquake Eng.*, 16(7–8), 495–502.
- Huston, D. R., Fuhr, P. L., Ambrose, T. P., and Barker, D. A. (1994). "Intelligent civil structures-activities in Vermont." *Smart Mater. Struct.*, 3(2), 129–139.
- Kammer, D. C. (1990). "Sensor placement for on-orbit modal identification and correlation of large space structures." *Proc., American Control Conf.*, IEEE, New York, 2984–2990.
- Laory, I., Hadj Ali, N. B., Trinh, T. N., and Smith, I. F. C. (2012). "Measurement system configuration for damage identification of continuously monitored structures." *J. Bridge Eng.*, 10.1061/(ASCE)BE.1943-5592.0000386, 857–866.
- Li, B., Ou, J., Zhao, X., and Li, D. (2011). "Optimal sensor placement in health monitoring system of Xinghai bay bridge." *Int. Workshop on Advanced Smart Materials and Smart Structures Technology*, DEStech Publications, Lancaster, PA.
- Li, D. S., Li, H. N., and Fritzen, C. P. (2007). "The connection between effective independence and modal kinetic energy methods for sensor placement." *J. Sound Vib.*, 305(4–5), 945–955.
- Lynch, J. P., and Loh, K. J. (2006). "A summary review of wireless sensors and sensor networks for structural health monitoring." *Shock Vib. Digest*, 38(2), 91–128.
- Meo, M., and Zumpano, G. (2005). "On the optimal sensor placement techniques for a bridge structure." *Eng. Struct.*, 27(10), 1488–1497.
- Middleton, D. (1960). *An introduction to statistical communication theory*, McGraw Hill, New York.
- Morassi, A., and Tonon, S. (2008). "Dynamic testing for structural identification of a bridge." *J. Bridge Eng.*, 10.1061/(ASCE)1084-0702(2008)13:6(573), 573–585.
- Pakzad, S. N., and Fenves, G. L. (2009). "Statistical analysis of vibration modes of a suspension bridge using spatially dense wireless sensor network." *J. Struct. Eng.*, 10.1061/(ASCE)ST.1943-541X.0000033, 863–872.
- Pandit, S. M. (1991). *Modal and spectrum analysis*, Wiley, New York.
- Papadimitriou, C. (2004). "Optimal sensor placement methodology for parametric identification of structural systems." *J. Sound Vibrat.*, 278(4–5), 923–947.
- Papadopoulos, M., and Garcia, E. (1998). "Sensor placement methodologies for dynamic testing." *AIAA J.*, 36(2), 256–263.
- Sacks, J., Welch, W. J., Mitchell, T. J., and Wynn, H. P. (1989). "Design and analysis of computer experiments." *Stat. Sci.*, 4(4), 409–423.
- Saitta, S., Kripakaran, P., Raphael, B., and Smith, I. F. (2008). "Improving system identification using clustering." *J. Comput. Civ. Eng.*, 10.1061/(ASCE)0887-3801(2008)22:5(292), 292–302.
- SAP2000 [Computer software]. Walnut Creek, CA, Computers and Structures (CSI).
- SMIT 1.0 [Computer software]. Bethlehem, PA, Lehigh Univ., ATLSS Engineering Center.
- Spencer, B. F., Jr., Ruiz-Sandoval, M. E., and Kurata, N. (2004). "Smart sensing technology: Opportunities and challenges." *J. Struct. Control Health Monit.*, 11(4), 349–368.
- Worden, K., and Burrows, A. P. (2001). "Optimal sensor placement for fault detection." *Eng. Struct.*, 23(8), 885–901.
- Yao, L., Sethares, W. A., and Kammer, D. C. (1992). "Sensor placement for on-orbit modal identification of large space structure via a genetic algorithm." *IEEE Int. Conf. on Systems Engineering*, IEEE, New York, 332–335.